ACCOUNTS of chemical research

Article

Cite This: Acc. Chem. Res. 2018, 51, 202−211

pubs.acs.org/accounts

Narrow Band Gap Conjugated Polyelectrolytes

Qiuhong Cui[†] and Guillermo C. Bazan*[,‡]

[†]Department of Physics, School of Science, Beijing Jiaotong University, Beijing 100044, P. R. China

[‡]Center for Polymers and Organic Solids, Departments of Chemistry & Biochemistry and Materials, University of California, Santa Barbara, Santa Barbara, California 93106, United States

CONSPECTUS: Two essential structural elements define a class of materials called conjugated polyelectrolytes (CPEs). The first is a polymer framework with an electronically delocalized, π-conjugated structure. This component allows one to adjust desirable optical and electronic properties, for example the range of wavelengths absorbed, emission quantum yields, electron affinity, and ionization potential. The second defining feature is the presence of ionic functionalities, which are usually linked via tethers that can modulate the distance of the charged groups relative to the backbone. These ionic groups render CPEs distinct relative to their neutral conjugated polymer counterparts. Solubility in polar solvents, including aqueous media, is an immediately obvious difference. This feature has enabled the development of optically amplified biosensor protocols and the fabrication of multilayer organic semiconductor devices through deposition techniques using solvents with orthogonal properties. Important but less obvious potential advantages must also be considered. For example, CPE layers have been used to introduce interfacial dipoles and thus modify the effective work function of adjacent electrodes. One can thereby modulate the barriers for charge injection into semiconductor layers and improve the device efficiencies of organic light-emitting diodes and solar cells. With a hydrophobic backbone and hydrophilic ionic sites, CPEs can also be used as dispersants for insoluble materials.

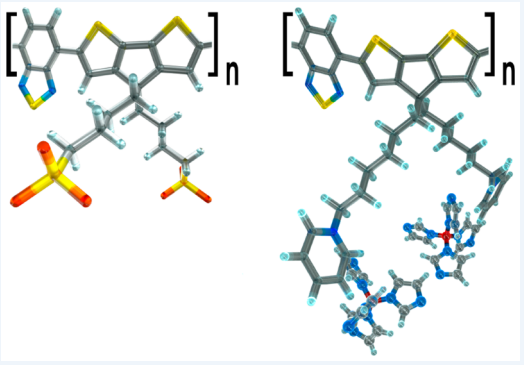

Narrow band gap CPEs (NBGCPEs) have been studied only recently. They contain backbones that comprise electron-rich and electron-poor fragments, a combination that leads to intramolecular charge transfer excited states and enables facile oxidation and reduction. One particularly interesting combination is NBGCPEs with anionic sulfonate side groups, for which spontaneous self-doping in aqueous media is observed. That no such doping is observed with cationic NBGCPEs indicates that the interplay between electrostatic forces and the redox chemistry of the organic semiconducting chain is essential for stabilizing the polaronic states and increasing the conductivity of the bulk. Capitalizing upon the properties of NBGCPEs has resulted in a range of new applications. When doped, they can be introduced as interlayers in organic and perovskite solar cells. Single-walled carbon nanotubes can be n- or p-doped with NBGCPEs, depending on whether the same backbone contains attached cationic or anionic side groups, respectively. The resulting dispersions can be used to fabricate flexible thermoelectric devices in which the n- and p-semiconductor legs are nearly identical in terms of chemical composition. Electrostatic interactions with negatively charged cell walls, in combination with the long-wavelength absorption and high photothermal efficiencies, have been used to create effective agents for photothermal killing of bacteria. Additionally, recent results have shown that cationic NBGCPEs can effectively n-dope graphene and that this doping is temperature-dependent. The preferential charge carriers can therefore be chosen to be electrons or holes depending on the applied temperature.

1.1. General Introduction to Narrow Band Gap Conjugated Polyelectrolytes

Conjugated polyelectrolytes (CPEs) are defined by a structure containing a π-conjugated backbone bearing pendant ionic groups.[1−5] The fact that CPEs combine the properties of organic semiconductors with the possibility of tuning the physical behavior by Coulombic forces has led to their integration into different technologies. For instance, CPEs in aqueous media have been used as optical reporters in biosensors and bioimaging applications.[6−11] Their solubility in polar solvents provides greener alternatives for the replacement of toxic solvents and makes it possible to fabricate multilayer optoelectronic devices in combination with nonpolar (nonionic) conjugated polymers. CPE interlayers prepared in this fashion have been integrated into organic photovoltaic (OPV) devices,[12−15] organic light-emitting diodes (OLEDs),[16−18] and organic thin-film transistors (OTFTs).[19,20] It is also worth noting that because they are amphiphilic, CPEs may also be considered as special surfactants that allow the introduction of an optoelectronically active element.[6] This feature provides the basis for their use as dispersants of other electronic materials, such as carbon nanotubes[21] and graphene.[22,23]

Their broad applications space has promoted the design and synthesis of a wide variety of CPEs through structural

Received: October 8, 2017
Published: December 14, 2017

DOI: 10.1021/acs.accounts.7b00501
Acc. Chem. Res. 2018, 51, 202−211

Scheme 1. (a) Synthesis of PCPDTBT-Pyr$^+$BIm$_4^-$; (b) Synthesis of PCPDTBTSO$_3$K and Conversion into PCPDTBTSO$_3$TBA[a]

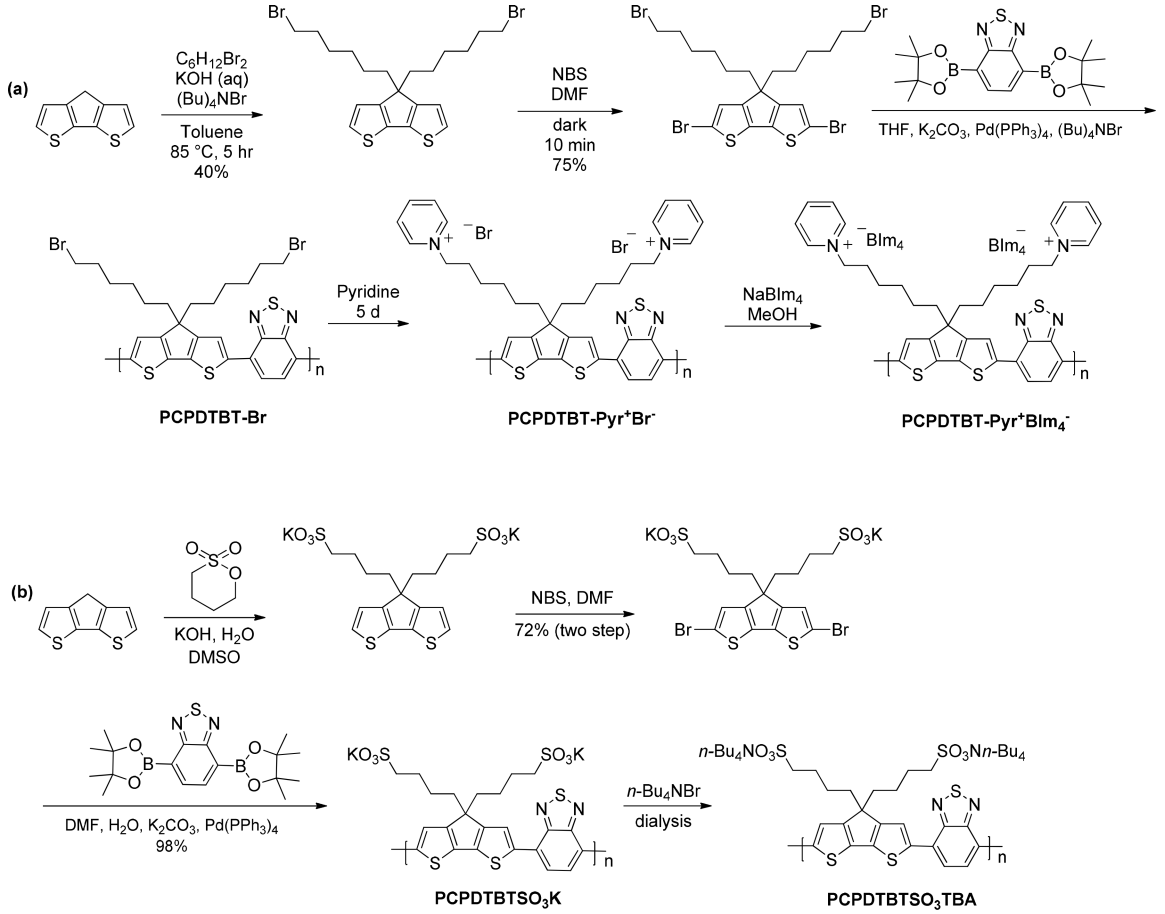

[a]Scheme 1a is adapted from ref 27. Copyright 2013 American Chemical Society. Scheme 1b is adapted with permission from ref 28. Copyright 2013 Wiley.

modifications of the backbone, tethered groups, ionic functionalities, and counterions. The π-conjugated element determines the primary optical properties of interest,[24] including absorption and emission spectra, light-harvesting capability (i.e., oscillator strength), transition moment orientation,[25] intrachain and interchain energy transfer, and emission quantum yield. One finds adaptation of structural units commonly found in typical neutral polymers, such as fluorene, phenylenevinylene, thiophene, electron-deficient heterocyclic units, and the like. Side groups allow one to modulate the average distance between the backbone and the charged units.[26] Charged groups may be cationic[27] or anionic,[28] a feature that can be used to predetermine preferential interactions with charged surfaces. Local electrostatic fields generated by the ionic units have also led to interesting observations in terms of charge transfer state stabilization and changes in exciton binding energies. Finally, counterions that compensate for the charge of the groups attached to the CPE are also relevant structural handles.[26] For example, it has been shown that a cationic CPE with smaller counteranions transports charge carriers more readily because of more intimate interchain interactions.[29,30]

Despite the research activity summarized above, the optical, physical, and electronic properties of narrow band gap CPEs (NBGCPEs) have been relatively unexplored. This absence is particularly noteworthy in view of the extraordinary efforts dedicated to the design of neutral NBG conjugated polymers for the fabrication of organic solar cells.[31−33] Although efforts in NBGCPE design have only recently emerged, the resulting materials have demonstrated unexpected features that are relevant for the design of self-doped conjugated polymers, organic thermoelectric materials, hybrid optoelectronic systems, and agents for the photothermal killing of bacteria. In this Account, we provide a perspective on the work carried out in our laboratories on NBGCPEs during the last 5 years, with an emphasis on how molecular structure impacts the doping of the materials and their possible applications.

1.2. Synthesis and Properties of NBGCPEs

One of our first objectives was the synthesis of the cationic NBGCPE PCPDTBT-Pyr$^+$BIm$_4^-$ (see Scheme 1a for chemical structures and their preparation).[27] Briefly, Suzuki copolymerization of an alkyl bromide-substituted dibromocyclopentadithiophene and the bis(boronic ester) of benzothiadiazole yields PCPDTBT-Br, which is uncharged. Postpolymerization quaternization with pyridine generates the cationic groups PCPDTBT-Pyr$^+$Br$^-$. As a final chemical modification, the bromide counterions in PCPDTBT-Pyr$^+$Br$^-$ can be exchanged with tetrakis(1-imidazolyl)borate anion (BIm$_4^-$) to provide PCPDTBT-Pyr$^+$BIm$_4^-$. BIm$_4^-$ counterions were introduced because of the higher solubility of the material and previous results incorporating CPEs as electron injection layers.[3,30,34]

We also synthesized anionic analogues of PCPDTBT-Pyr$^+$BIm$_4^-$ with charges provided through the presence of

DOI: 10.1021/acs.accounts.7b00501
Acc. Chem. Res. 2018, 51, 202−211

sulfonate groups (Scheme 1b).[28] Alkylation of cyclopentadithiophene (CPDT) with 1,4-butanesultone followed by bromination using *N*-bromosuccinimide (NBS), provides monomer **1**. Coupling of **1** and bispinacolate **2** under Suzuki reaction conditions affords PCPDTBTSO$_3$K. Cation exchange procedures provide PCPDTBTSO$_3$TBA, in which the original potassium countercations are replaced with tetrabutylammonium (TBA) in order to increase the solubility in organic solvents.

Figure 1 shows the optical absorption spectra of PCPDTBTSO$_3$K in water obtained before and after a standard dialysis purification procedure used to remove salts from the polymerization reaction. Most relevant is the emergence after dialysis of a broad, low-energy transition observed from 900 to 1300 nm, which is reminiscent of what is observed for polarons, i.e., radical cations. One finds that by adding acid or base, one can modulate the contribution from the low-energy band, as shown in Figure 2. The 1150 nm peak increases upon addition of 10 equiv of HCl (Figure 2a) and is absent when 10 equiv of KOH is added (Figure 2c). The electron paramagnetic resonance (EPR) spectra in Figure 2b,d are also consistent with the formation of a doped chain.

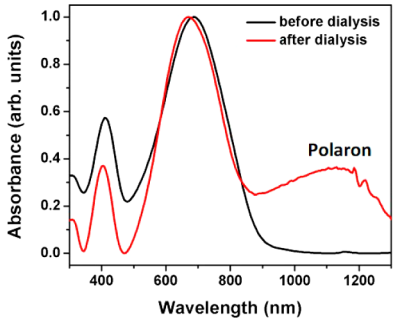

Figure 1. UV/vis/NIR absorption spectra of PCPDTBTSO$_3$K in water before and after dialysis. Adapted with permission from ref 28. Copyright 2013 Wiley.

To examine the role of electrostatic contributions by adjacent ions while maintaining the backbone structure constant, we compared PCPDTBT-Pyr$^+$BIm$_4^-$ with PCPDTBTSO$_3$K and PCPDTBTSO$_3$TBA. The latter was obtained through ion exchange procedures previously developed in our laboratories.[28] In the presence of base, the absorption of PCPDTBT-Pyr$^+$BIm$_4^-$ is similar to what is observed with PCPDTBTSO$_3$K in the presence of base. However, no changes are observed when 50 equiv of HCl is added to PCPDTBT-Pyr$^+$BIm$_4^-$. By analogy to previous studies on self-doped polymers, it is reasonable that doping during dialysis proceeds via a mechanism that involves protonation of the polymer chain.[35] However, the difference between PCPDTBTSO$_3$K and PCPDTBT-Pyr$^+$BIm$_4^-$ indicates that the anionic groups play a critical role in stabilizing the (cationic) polaronic states, and this most simply appears to occur as a result of the differences in electrostatic stabilization by the charges on the backbone (see Figure 3).

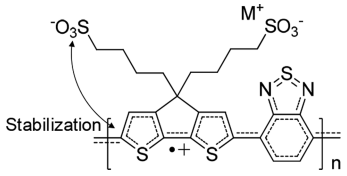

Figure 3. Electrostatic stabilization of the polaron (radical cation) by adjacent anionic sulfonate groups.

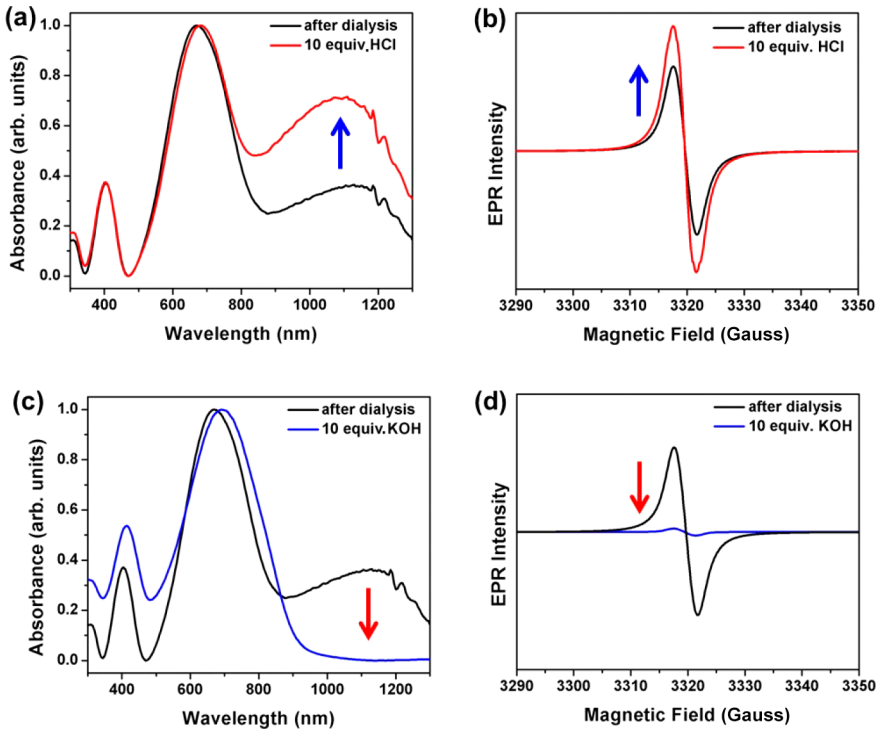

Figure 2. (a, c) UV/vis/NIR absorption spectra of PCPDTBTSO$_3$K in solution after dialysis with 10 equiv of (a) HCl or (c) KOH added. (b, d) EPR signals after dialysis with 10 equiv of (b) HCl of (d) KOH added. Adapted with permission from ref 28. Copyright 2013 Wiley.

DOI: 10.1021/acs.accounts.7b00501
Acc. Chem. Res. 2018, 51, 202−211

To probe how the different structural units come together to favor the doping process, we examined $PFBTSO_3Na$ (Figure 4), in which the CPDT unit in $PCPDTBTSO_3K$ is replaced

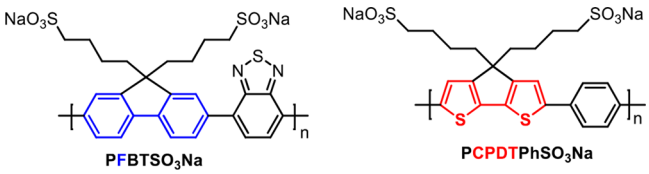

Figure 4. Chemical structures of $PFBTSO_3Na$ and $PCPDTPhSO_3Na$.

with a fluorene fragment, which is a weaker donor. Regardless of the treatment, one does not observe any indication of doping, thereby illustrating the key role played by the CPDT unit. Furthermore, $PCPDTPhSO_3Na$ (Figure 4), which contains a structure comprising alternating CPDT and phenylene units, can indeed be self-doped. CPDT is categorized as a strong donor for the design of narrow band gap polymers, which implies a low ionization potential, a feature that favors the formation of radical cations.

A series of anionic NBGCPEs were prepared to gauge relevant properties as functions of the counterion and the length of the tether linking the sulfonate groups to the main chain while keeping the backbone features constant (Figure 5). Figure 5c shows that the UV/vis/NIR absorptions of the CPE films confirm their doped states, as determined by the presence of transitions centered around 1250 nm and extending to lower energies. Shorter side chains translate into increased doping, higher crystallinity, and preferential edge-on orientation, all of which may be used to modulate the charge carrier transport characteristics. As shown by grazing-incidence wide-angle X-ray scattering (GIWAXS) (Figure 6), smaller counterions (Na^+ and K^+ vs TBA) lead to tighter $\pi-\pi$ interaction and higher levels of crystallinity, which may be responsible for the higher electrical conductivities.[26]

2. NBGCPES AS CHARGE TRANSPORT/RECOMBINATION INTERLAYERS

Organic field-effect transistor (OFET) devices fabricated with PCPDTBT-Br (see Scheme 1) showed typical p-type transistor

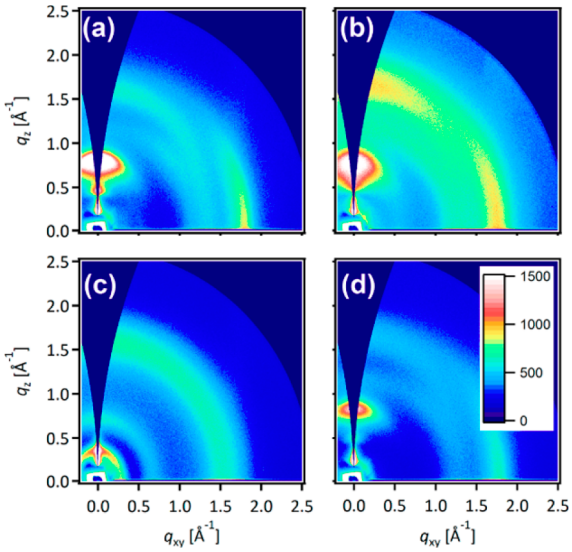

Figure 6. Two-dimensional GIWAXS patterns of thin films on silicon substrates: (a) $PCPDTBTSO_3Na$ (CPE-Na), (b) $PCPDTBTSO_3K$ (CPE-K), (c) $PCPDTBTSO_3TBA$ (CPE-TBA), and (d) $PCPDTBTSO_3$-C3-K (CPE-C3-K). Adapted from ref 26. Copyright 2014 American Chemical Society.

behavior, while those using $PCPDTBT\text{-}Pyr^+BIm_4^-$ exhibited n-type behavior (Figure 7). It is worth pointing out, however, that UV photoemission spectroscopy (UPS) measurements show a lowering of both the LUMO and HOMO energy levels for $PCPDTBT\text{-}Pyr^+BIm_4^-$ relative to PCPDTBT-Br. Additionally, the absorption maximum of $PCPDTBT\text{-}Pyr^+BIm_4^-$ is shifted to longer wavelengths, a feature that suggests stabilization of intramolecular charge transfer states by the electrostatic field. One possible scenario for the n-type behavior of $PCPDTBT\text{-}Pyr^+BIm_4^-$ is that the charged groups generate interfacial electrostatic dipoles that decrease the barriers for injection of charges.[13] However, depositing a thin layer of $PCPDTBT\text{-}Pyr^+BIm_4^-$ atop PCPDTBT-Br does not provide a similar effect. These observations suggest that interfacial effects alone may not provide the complete picture for realizing n-type FET transport. Another possibility is that the lowering of the orbital energy levels stabilizes the radical anion (polaron), a feature

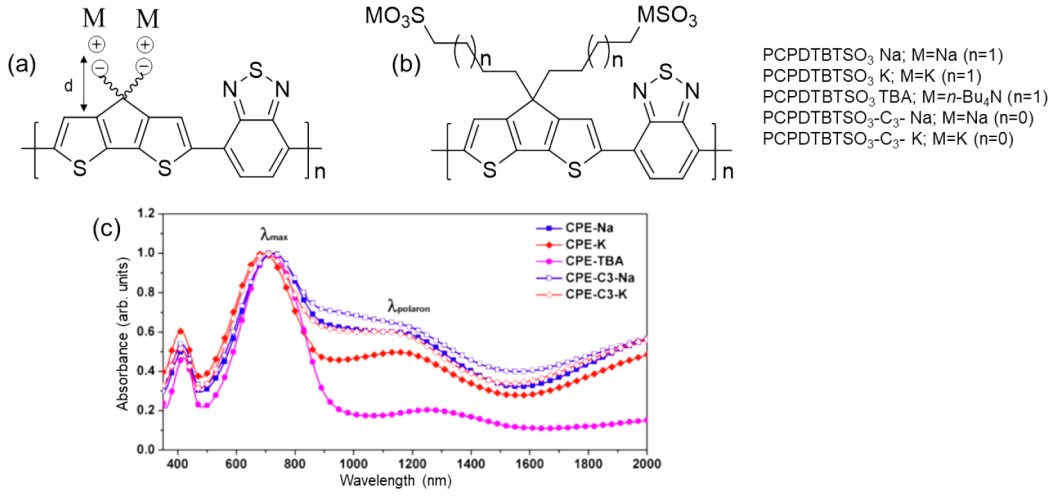

Figure 5. (a) Representations of molecules with different counterions and alkyl side chain lengths. (b) Chemical structures of the CPEs studied. (c) Thin-film absorptions, normalized to λ_{max}, of CPEs on glass substrates. Adapted from ref 26. Copyright 2014 American Chemical Society.

DOI: 10.1021/acs.accounts.7b00501
Acc. Chem. Res. 2018, 51, 202−211

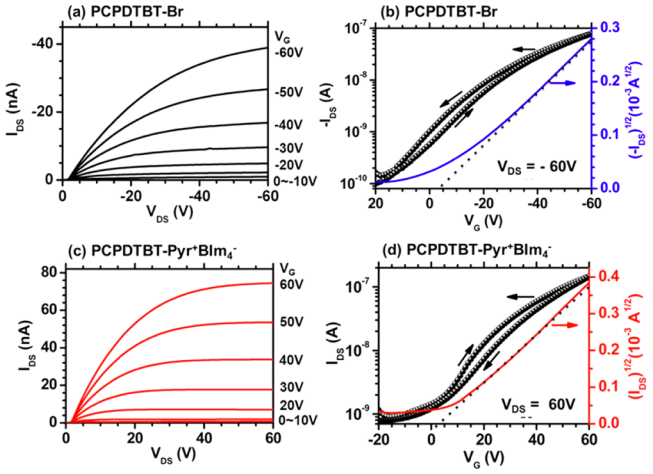

Figure 7. OFET characteristics with transport layers of (a, b) PCPDTBT-Br and (c, d) PCPDTBT-Pyr$^+$BIm$_4^-$. The hole mobility for PCPDTBT-Br was 6×10^{-5} cm^2 V^{-1} s^{-1}, and the electron mobility for PCPDTBT-Pyr$^+$BIm$_4^-$ was -1×10^{-4} cm^2 V^{-1} s^{-1}. Adapted from ref 27. Copyright 2013 American Chemical Society.

unavailable for neutral polymers with identical backbone repeat units.

As shown in Figure 8, the electrical conductivity of PCPDTBTSO$_3$K (~1.2 S cm^{-1}) is comparable to that of

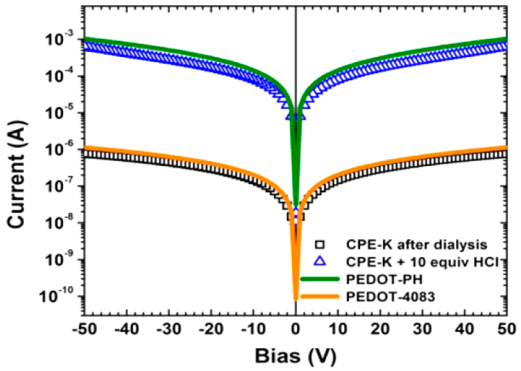

Figure 8. Current–voltage plot of thin films of PCPDTBTSO$_3$K after dialysis, PCPDTBTSO$_3$K with 10 equiv of HCl added, PEDOT-4083, and PEDOT-PH. Adapted with permission from ref 28. Copyright 2013 Wiley.

commercially available poly(3,4-ethylenedioxythiophene):poly(styrenesulfonate) (PEDOT:PSS) (~2.0 S cm^{-1}). However, the fact that PEDOT:PSS is acidic raises the potential to introduce interfacial reactions that may limit device performance with organic semiconductors with basic functional units.[36−40] We therefore used PCPDTBTSO$_3$K as-obtained after dialysis as a hole transport layer in organic solar cells and were pleased to find performance similar to that of solar cells containing PEDOT:PSS.[41] From the current density–voltage (J–V) curves shown in Figure 9a, devices with a PCPDTBTSO$_3$K hole transport layer (HTL) achieve a power conversion efficiency (PCE) of 8.2% with a larger short-circuit current (J_{sc}), a better fill factor (FF), and a smaller open-circuit voltage (V_{oc}) relative to PEDOT:PSS-containing devices. The minor decrease in V_{oc} was attributed to a shallower HOMO for PCPDTBTSO$_3$K (~4.9 eV) relative to PEDOT:PSS (~5.0 eV). Moreover, PCPDTBTSO$_3$K HTLs also demonstrated success in the fabrication of small-molecule bulk-heterojunction cells (with the small-molecule donor p-DTS(FBTTh$_2$)$_2$). As shown in Figure 9b, incorporation of the PCPDTBTSO$_3$K interlayer in p-DTS(FBTTh$_2$)$_2$:PC$_{71}$BM active layers leads to a PCE of 7.2%, which is similar to that using PEDOT:PSS HTLs (7.1%). These results showed that water/alcohol-soluble CPEs can be used as efficient HTLs, which contrasts their predominant application to facilitate electron injection.

To further demonstrate relevance to organic solar cells, we point out that tandem solar cells require the insertion of low-loss interconnection layers (ICLs) between the two subcells. ICLs generally comprise a p-type HTL and an n-type electron transport layer (ETL). The layer promotes charge recombination and at the same time serves to shift the vacuum level. As shown in Figure 10a, a tandem device structure was fabricated with the general architecture indium tin oxide (ITO)/PEDOT:PSS/PTB7-Th:PC$_{71}$BM/ZnO/PCPDTBTSO$_3$K or PCPDTPhSO$_3$Na/PTB7-Th:PC$_{71}$BM/Al.[42] The molecular structures of PCPDTBTSO$_3$K (CPE-K) and PCPDTPhSO$_3$Na (CPEPh-Na) are shown in Figure 10b,c. The work function of the HTL plays a significant role in hole extraction and affects charge recombination within the ICL. The optimized tandem cells with a ZnO/PCPDTPhSO$_3$Na ICL reached a PCE of 11.3% (Figure 10d), a 25% improvement compared with single cells.

PCPDTBT-K was also successfully employed in inverted-type perovskite solar cells by using the simple architecture ITO/PCPDTBTSO$_3$K/MAPbI$_{3-x}$Cl$_x$ perovskite/PCBM/Al. The perovskite precursor solution wets nicely atop

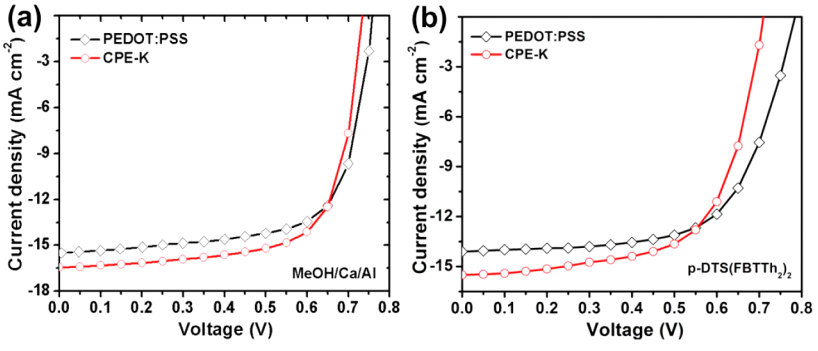

Figure 9. (a) J–V curves of PTB7:PC$_{71}$BM solar cells using PEDOT:PSS or PCPDTBTSO$_3$K (CPE-K) (8 nm) HTLs and a Ca/Al cathode with methanol treatments. (b) J–V curves of p-DTS(FBTTh$_2$)$_2$:PC$_{71}$BM solar cells incorporating PEDOT:PSS or PCPDTBTSO$_3$K (CPE-K) HTLs under 100 mW cm^{-2} irradiation. Adapted with permission from ref 41. Copyright 2013 Wiley.

DOI: 10.1021/acs.accounts.7b00501
Acc. Chem. Res. 2018, 51, 202−211

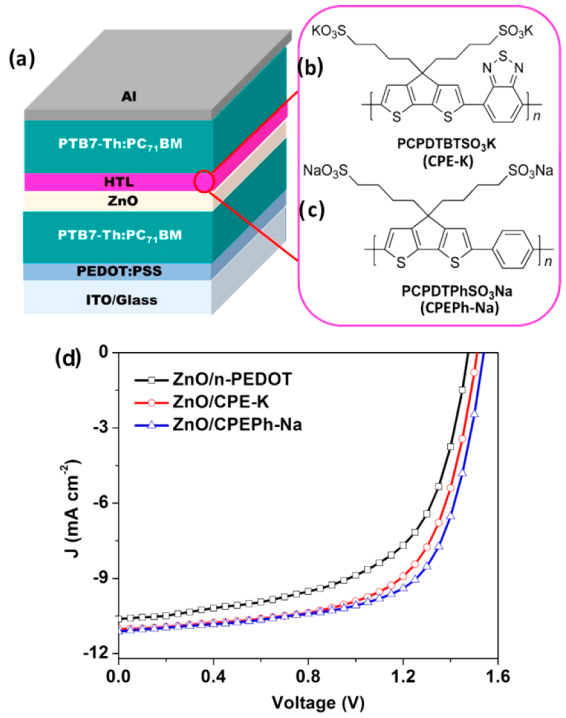

Figure 10. (a) Device structure of tandem cells. (b, c) Molecular structures of two different HTLs: (b) $PCPDTBTSO_3K$ (CPE-K) and (c) $PCPDTPhSO_3Na$ (CPEPh-Na). (d) *J*–*V* characteristics of single cells with different HTLs. Adapted with permission from ref 42. Copyright 2015 Wiley.

$PCPDTBTSO_3K$, thereby leading to a uniform active layer with complete surface coverage and appropriate hole selectivity for facilitating transport to the anode. Under these conditions, the device with $PCPDTBTSO_3K$ exhibits a higher device efficiency (>12%) compared with the device fabricated with widely used PEDOT:PSS (9.4%).[43] Of interest is the observation that $PCPDTBTSO_3K$ improved the stability of devices in air, presumably because of its neutral pH (Figure 11). As an alternative to PEDOT:PSS and p-type metal oxides, $PCPDTBTSO_3K$ thereby provides a new basis for designing hole transport materials for efficient perovskite/fullerene solar cells.

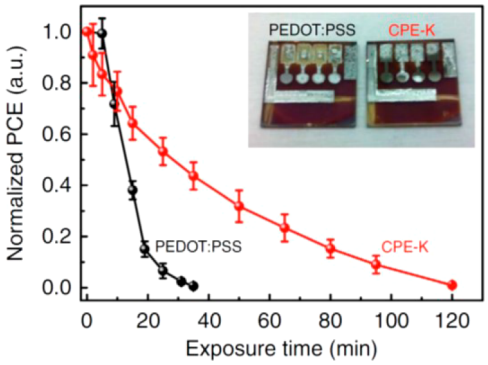

Figure 11. Device stability of perovskite solar cells with PEDOT:PSS and $PCPDTBTSO_3K$ (CPE-K) under ambient air conditions. The insets are photographs of real devices with PEDOT:PSS and $PCPDTBTSO_3K$ (CPE-K) after air exposure for 12 h. PCE refers to the power conversion efficiency. Adapted with permission from ref 43. Copyright 2015 Nature Publishing Group.

3. NBGCPES AS ANTIMICROBIAL MATERIALS

Conventional CPEs have been used in antimicrobial applications.[44−47] Structures with quaternary ammonium side chains have shown high antimicrobial activities against different bacteria.[48,49] However, most CPEs are characterized by absorption within the visible region of the spectrum. Shifting the transition energies to the near-infrared (NIR) region would be expected to provide deeper penetration of light and enable optically triggered antimicrobial function. NBGCPEs are able to meet such requirements.

Two NBGCPEs with similar backbones but differing in the charge appended to the backbone were compared within the context of binding affinity toward bacteria and photothermal conversion efficiencies, as shown in Figure 12a.[50] The zeta

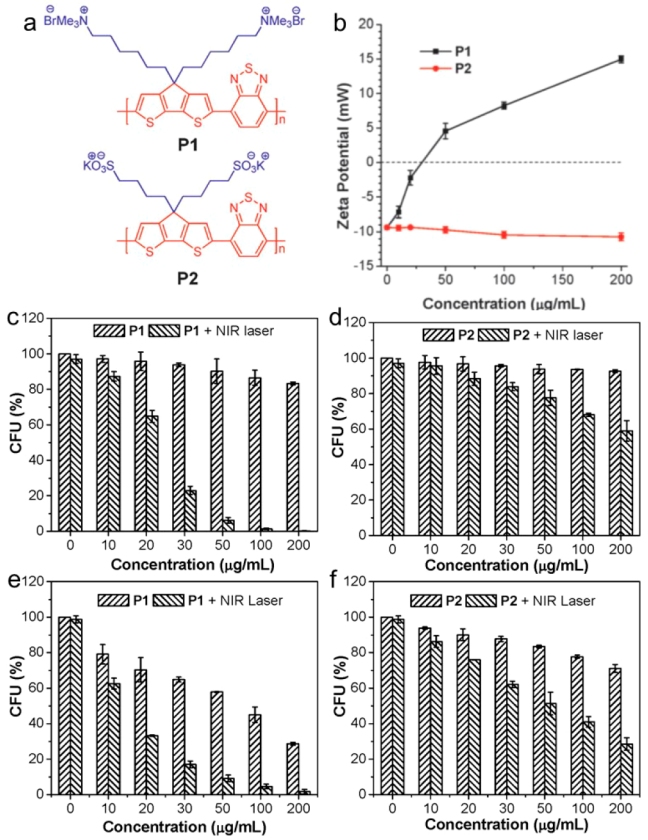

Figure 12. (a) Chemical structures of $PCPDTBTNMe_3Br$ (P1) and $PCPDTBTSO_3K$ (P2). (b) Zeta potential changes of P1- or P2-treated *Escherichia coli* at various concentrations. (c–f) Survival percentages of (c, d) *E. coli* and (e, f) *Bacillus subtilis* after treatment with (c, e) P1 or (d, f) P2. Adapted with permission from ref 50. Copyright 2015 Royal Society of Chemistry.

potential measurements in Figure 12b show that cationic $PCPDTBTNMe_3Br$ (P1) binds with high affinity to bacteria. In contrast, its anionic analogue $PCPDTBTSO_3K$ (abbreviated as P2 in the original publication) exhibits low binding affinity. The high affinity of $PCPDTBTNMe_3Br$ toward bacteria is attributed to electrostatic binding to the negatively charged cell; little contribution from hydrophobic interactions was detected. These features, together with excellent light-to-heat conversion ability under NIR laser irradiation, make $PCPDTBTNMe_3Br$ an excellent bactericidal reagent (see the survival percentages provided in Figure 12c–f). These results reveal opportunities for further design of photothermal CPEs, which may be

DOI: 10.1021/acs.accounts.7b00501
Acc. Chem. Res. 2018, 51, 202−211

functionalized with antibodies, aptamers, or other recognition fragments to specifically bind cancer cells for treatment and related theranostic applications.

4. NBGCPES AS THERMOELECTRIC MATERIALS

Thermoelectric materials are predominantly inorganic semiconductors;[51] inorganic/organic combinations have also been examined.[52,53] Organic materials have gathered recent interest[54−57] because of their low thermal conductivity, structural variations, and ease of processing.[58] For example, PEDOT:Tos (Tos = tosylate) can be processed to have a power factor, $S^2\sigma$, of ~450 μW/m K^2, where S is the Seebeck coefficient and σ is the electrical conductivity. Because of the locally available charge-compensating ions and relatively well-defined structures, self-doped CPEs are relevant candidates for thermoelectric materials, particularly within the context of developing structure−function relationships. Thus, a series of anionic NBGCPEs with CPDT-*alt*-BT repeat units but with different counterions and modified alkyl side chains were studied. General trends obtained from these studies include the following. CPEs with smaller counterions exhibit better conductivities with diminished thermopowers, most reasonably because of the more pronounced doping, tighter $\pi-\pi$ interaction, and higher level of crystallinity in the films. Shorter linkers lead to increased levels of doping, better crystallinity, and a more edge-on molecular orientation, thereby providing handles to modulate σ. The main point of these studies is that they reveal the diversity of structural handles that may be used in CPEs to tailor the thermoelectric performance of a given conjugated backbone.

5. HYBRID MATERIALS CONTAINING NBGCPES

Solubility in aqueous media enables CPEs to be effective dispersants for hydrophobic materials, such as carbon nanotubes (CNTs).[59,60] Unlike conventional surfactants, NBGCPEs can be used to incorporate a semiconducting or conducting component into the resulting composite blend. As a point of demonstration, we selected PCPDTBTSO$_3$TBA to disperse single-walled carbon nanotubes (SWNTs). The electrical conductivity of the composite films was analyzed through conductive atomic force microscopy (c-AFM) (Figure 13). For comparison, we also studied PCPDTBTPyr$^+$BIm$_4^-$:SWNT and a dispersion containing poly(sodium 4-styrenesulfonate) (PSSNa):SWNT. As-cast PCPDTBTSO$_3$TBA:SWNT composites are more conductive than PCPDTBTPyr$^+$BIm$_4^-$:SWNT composites, most reasonably because of a higher density of unpaired free electrons; both composites have higher electrical conductivity than PSSNa:SWNT. SWNT composite films for both PCPDTBTSO$_3$TBA and PCPDTBTPyr$^+$BIm$_4^-$ can be further enhanced by treatment with CF_3CO_2H vapor. Since PSSNa does not dope with acid, these studies highlight the multifaceted function of doped NBGCPEs: acting as dispersants and incorporating interfacial agents that improve charge transport.

SWNT composites are typically characterized by p-type behavior.[62−64] For organic electronics one finds the need for both p-type and n-type semiconductors. Having a set of complementary NBGCPEs allowed us to examine how they dope SWNTs by measuring σ and S. The type of the doping is indicated by the sign of S, for which positive and negative signs indicate p- and n-type charge transport, respectively. Specifically, NBGCPEs with cationic or anionic functionalities provide

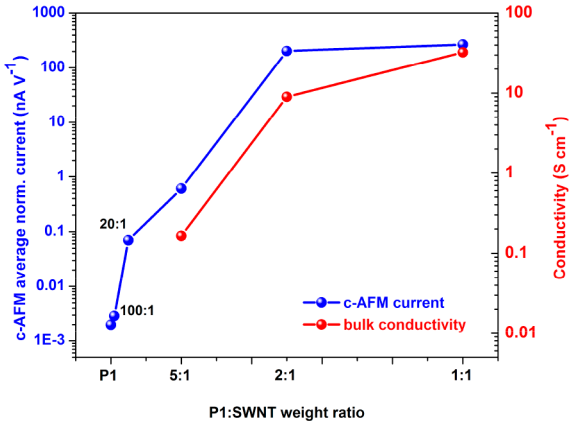

Figure 13. Comparison of the trend in the c-AFM average current for a PCPDTBTSO$_3$TBA (P1) film and P1:SWNT composite films with different weight ratios and the trend in the conductivity measured using a four-point probe for P1:SWNT composite films with different weight ratios. Adapted with permission from ref 61. Copyright 2014 Wiley.

n-type or p-type conductive NBGCPE/SWNT composites, respectively, at nonexcess loadings of SWNTs. Using PCPDTBTSO$_3$Na as the dispersing agent leads to composites with relatively high conductivity, most reasonably because of the minimization of inter-SWNT contact resistance. Cationic NBGCPE/SWNT composites exhibit negative S (Figure 14a). Both p- and n-type NBGCPE/SWNT composites were used to fabricate flexible thermoelectric modules (Figure 14c,d).[65,66] These NBGCPE/SWNT composites open opportunities for processing from water using various solution deposition techniques.

The observation that cationic PCPDTBT-Pyr$^+$BIm$_4^-$ is capable of n-doping SWNTs led us to probe whether a similar effect could be induced on well-defined single-layer chemical vapor deposition (CVD) graphene sheets. Indeed, using a combination of Hall effect measurements, determination of Seebeck coefficients, and transport in field-effect transistors, it was determined that a submonolayer of PCPDTBT-Pyr$^+$BIm$_4^-$ leads to graphene transport of holes or electrons as a function of temperature. Specifically, the temperature-dependent Hall effect on the heterobilayer nanocomposites provides information on how n- and p-type transport mechanisms respond to heating or cooling. Figure 15a,b shows the Hall coefficient (R_H) and the sheet resistance of the PCPDTBT-Pyr$^+$BIm$_4^-$/graphene nanocomposites as functions of temperature.[67] The n-type doping efficiencies of both the thick and thin CPEPyrBIm$_4$ layers decrease with increasing temperature since the absolute value of R_H decreases. However, in the case of the thin heterobilayer, R_H changes sign from negative to positive at 331 K. Therefore, the type of conductivity as determined by the majority charge carriers is switchable by temperature. Moreover, the doping effect is reversible, albeit with significant hysteresis. The overall effect shows the unique and complex nature of the electrical properties of the novel heterobilayer hybrid organic/inorganic CPEPyrBIm$_4$/graphene nanocomposite material and enhances interest in further investigations to understand the complex chemistry and physics that are accessible through application of CPE interlayers.

DOI: 10.1021/acs.accounts.7b00501
Acc. Chem. Res. 2018, 51, 202−211

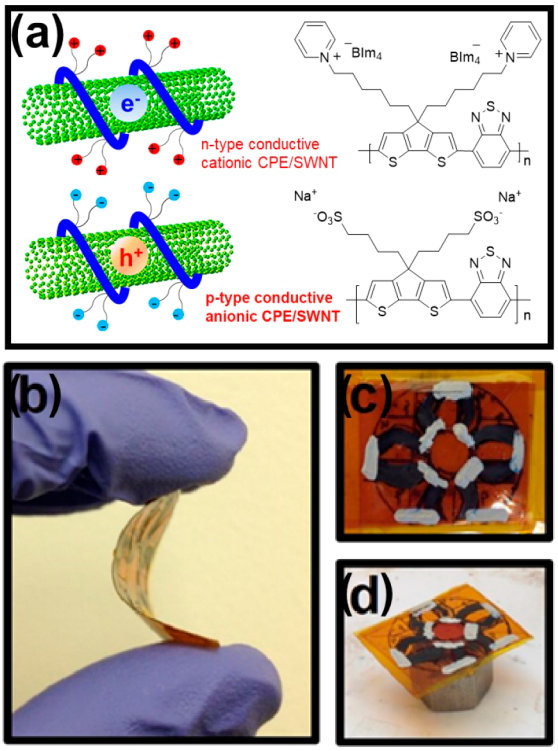

Figure 14. (a) Chemical structures of PCPDTBTSO$_3$Na and PCPDTBT-Pyr$^+$BIm$_4^-$, which respectively provide p- and n-type thermoelectric composites upon blending with SWNTs. (b) Deposition on a Kapton substrate enables module flexibility. (c) Thermoelectric generator constructed using PCPDTBTSO$_3$Na/SWNT (1:1) as p-type legs and PCPDTBT-Pyr$^+$BIm$_4^-$/SWNT (1:1) as n-type legs. (d) A flat-topped metal heating block provided the localized heating. Adapted with permission from ref 65. Copyright 2015 Royal Society of Chemistry.

6. CONCLUDING REMARKS AND FUTURE OUTLOOK

In this Account, we have described our recent work with NBGCPEs, with a particular emphasis on how the different structural modules can be put together to substantially influence the properties and function of the material. The role of electrostatics in modulation of self-doping in the polymer is, in our opinion, particularly noteworthy. Detailed structure−property relationships in hybrid materials have yet to emerge. Consider, for example, how little we know about the intimate contact between the NBGCPEs and SWNTs or graphene and the mechanism by which the preferred charge carrier changes with temperature in PCPDTBT-Pyr$^+$BIm$_4^-$/graphene bilayers. The exact doping mechanisms are likely impacted by the geometric relationships among the surface, the backbone, the pendant ionic functionalities, and the charge-compensating anions. How ion motion also perturbs charge transport remains to be fully studied. It is also likely that there is much to gain by incorporating biological recognition units to NBGCPEs with high photothermal conversion efficiencies in order to introduce elements of specificity. Despite these uncertainties, the fact that this relatively new class of materials has been incorporated into technologies ranging from solid-state optoelectronic devices to composites with tunable charge transport to photothermal antimicrobial techniques highlights the unique opportunities for further applications and discoveries.

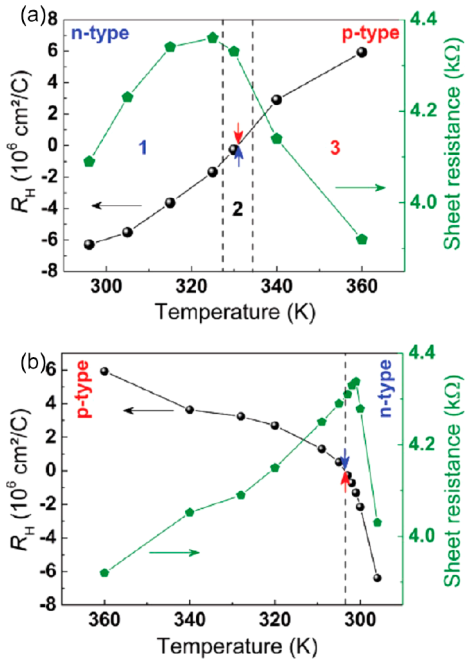

Figure 15. (a) Temperature dependence of the Hall coefficient (R_H) and the sheet resistance for a thin layer of PCPDTBT-Pyr$^+$BIm$_4^-$ on graphene (annealed at 373 K). (b) Temperature dependence of R_H and the sheet resistance for a thin PCPDTBT-Pyr$^+$BIm$_4^-$ layer on graphene while cooling. Adapted with permission from ref 67. Copyright 2017 Wiley.

AUTHOR INFORMATION

Corresponding Author

*E-mail: bazan@chem.ucsb.edu.

ORCID

Guillermo C. Bazan: 0000-0002-2537-0310

Notes

The authors declare no competing financial interest.

Biographies

Qiuhong Cui is an Assistant Professor at Beijing Jiaotong University. She received her Ph.D. in 2014 at the Institute of Chemistry, Chinese Academy of Sciences. She then joined Professor Bazan's group at UCSB as a visiting scholar from October 2015 to October 2016. Her research is focused on organic nanomaterials and their applications, including the synthesis of low-dimensional materials, comprehensive studies of the photochemical and optical processes in the resulting materials, and the design, fabrication, and optimization of optoelectronic nanodevices.

Guillermo C. Bazan is a Distinguished Professor in the Departments of Chemistry & Biochemistry and Materials and the Director of the Center for Polymers and Organic Solids at the University of California, Santa Barbara. He carried out his undergraduate studies at the University of Ottawa. His graduate work was done at MIT, working under the guidance of Professor Richard R. Schrock. His research efforts are dedicated toward the design of organic semiconducting materials for bioelectrochemical and solid-state device applications.

ACKNOWLEDGMENTS

This work was supported by the National Science Foundation (DMR 1411240) and the National Natural Science Foundation of China (51603010).

DOI: 10.1021/acs.accounts.7b00501
Acc. Chem. Res. 2018, 51, 202−211

REFERENCES

(1) Patil, A. O.; Ikenoue, Y.; Wudl, F.; Heeger, A. J. Water soluble conducting polymers. *J. Am. Chem. Soc.* **1987**, *109*, 1858−1859.

(2) Liu, B.; Bazan, G. C. *Conjugated Polyelectrolytes: Fundamentals and Applications*; Wiley-VCH: Weinheim, Germany, 2013.

(3) Hoven, C. V.; Garcia, A.; Bazan, G. C.; Nguyen, T. Q. Recent applications of conjugated polyelectrolytes in optoelectronic devices. *Adv. Mater.* **2008**, *20*, 3793−3810.

(4) Yang, T.; Wang, M.; Duan, C.; Hu, X.; Huang, L.; Peng, J.; Huang, F.; Gong, X. Inverted polymer solar cells with 8.4% efficiency by conjugated polyelectrolyte. *Energy Environ. Sci.* **2012**, *5*, 8208−8214.

(5) Lee, W.; Seo, J. H.; Woo, H. Y. Conjugated polyelectrolytes: A new class of semiconducting material for organic electronic devices. *Polymer* **2013**, *54*, 5104−5121.

(6) Hoven, C. V.; Garcia, A.; Bazan, G. C.; Nguyen, T.-Q. Recent applications of conjugated polyelectrolytes in optoelectronic devices. *Adv. Mater.* **2008**, *20*, 3793−3810.

(7) Schanze, K. S.; Shelton, A. H. Functional polyelectrolytes. *Langmuir* **2009**, *25*, 13698−13702.

(8) Jiang, H.; Taranekar, P.; Reynolds, J. R.; Schanze, K. S. Konjugierte polyelektrolyte: synthese, photophysik und anwendungen. *Angew. Chem.* **2009**, *121*, 4364−4381.

(9) Jiang, H.; Taranekar, P.; Reynolds, J. R.; Schanze, K. S. Conjugated polyelectrolytes: synthesis, photophysics, and applications. *Angew. Chem., Int. Ed.* **2009**, *48*, 4300−4316.

(10) Huang, F.; Wu, H.; Cao, Y. Water/alcohol soluble conjugated polymers as highly efficient electron transporting/injection layer in optoelectronic devices. *Chem. Soc. Rev.* **2010**, *39*, 2500−2521.

(11) Duarte, A.; Pu, K.-Y.; Liu, B.; Bazan, G. C. Recent advances in conjugated polyelectrolytes for emerging optoelectronic applications. *Chem. Mater.* **2011**, *23*, 501−515.

(12) Wu, Z.; Sun, C.; Dong, S.; Jiang, X.-F.; Wu, S.; Wu, H.; Yip, H.-L.; Huang, F.; Cao, Y. n-Type water/alcohol-soluble naphthalene diimide-based conjugated polymers for high-performance polymer solar cells. *J. Am. Chem. Soc.* **2016**, *138*, 2004−2013.

(13) Seo, J. H.; Gutacker, A.; Sun, Y.; Wu, H.; Huang, F.; Cao, Y.; Scherf, U.; Heeger, A. J.; Bazan, G. C. Improved high-efficiency organic solar cells via incorporation of a conjugated polyelectrolyte interlayer. *J. Am. Chem. Soc.* **2011**, *133*, 8416−8419.

(14) Sun, C.; Wu, Z.; Hu, Z.; Xiao, J.; Zhao, W.; Li, H.-W.; Li, Q.-Y.; Tsang, S.-W.; Xu, Y.-X.; Zhang, K.; Yip, H.-L.; Hou, J.; Huang, F.; Cao, Y. Interface design for high-efficiency non-fullerene polymer solar cells. *Energy Environ. Sci.* **2017**, *10*, 1784−1791.

(15) Hu, Z.; Xu, R.; Dong, S.; Lin, K.; Liu, J.; Huang, F.; Cao, Y. Quaternisation-polymerized N-type polyelectrolytes: synthesis, characterisation and application in high-performance polymer solar cells. *Mater. Horiz.* **2017**, *4*, 88−97.

(16) Hoven, C. V.; Yang, R.; Garcia, A.; Crockett, V.; Heeger, A. J.; Bazan, G. C.; Nguyen, T.-Q. Electron injection into organic semiconductor devices from high work function cathodes. *Proc. Natl. Acad. Sci. U. S. A.* **2008**, *105*, 12730−12735.

(17) Fang, J.; Wallikewitz, B. H.; Gao, F.; Tu, G.; Müller, C.; Pace, G.; Friend, R. H.; Huck, W. T. S. Conjugated zwitterionic polyelectrolyte as the charge injection layer for high-performance polymer light-emitting diodes. *J. Am. Chem. Soc.* **2011**, *133*, 683−685.

(18) Zhu, X.; Xie, Y.; Li, X.; Qiao, X.; Wang, L.; Tu, G. Anionic conjugated polyelectrolyte-wetting properties with an emission layer and free ion migration when serving as a cathode interface layer in polymer light emitting diodes (PLEDs). *J. Mater. Chem.* **2012**, *22*, 15490−15494.

(19) Seo, J. H.; Gutacker, A.; Walker, B.; Cho, S.; Garcia, A.; Yang, R.; Nguyen, T.-Q.; Heeger, A. J.; Bazan, G. C. Improved injection in n-type organic transistors with conjugated polyelectrolytes. *J. Am. Chem. Soc.* **2009**, *131*, 18220−18221.

(20) Seo, J. H.; Namdas, E. B.; Gutacker, A.; Heeger, A. J.; Bazan, G. C. Solution-processed organic light-emitting transistors incorporating conjugated polyelectrolytes. *Adv. Funct. Mater.* **2011**, *21*, 3667−3672.

(21) Li, Y.; Mai, C. K.; Phan, H.; Liu, X.; Nguyen, T. Q.; Bazan, G. C.; Chan-Park, M. B. Electronic properties of conjugated polyelectrolyte/single-walled carbon nanotube composites. *Adv. Mater.* **2014**, *26*, 4697−4703.

(22) Yang, H.; Zhang, Q.; Shan, C.; Li, F.; Han, D.; Niu, L. Stable, Conductive supramolecular composite of graphene sheets with conjugated polyelectrolyte. *Langmuir* **2010**, *26*, 6708−6712.

(23) Qi, X.; Pu, K.-Y.; Zhou, X.; Li, H.; Liu, B.; Boey, F.; Huang, W.; Zhang, H. Conjugated-polyelectrolyte-functionalized reduced graphene oxide with excellent solubility and stability in polar solvents. *Small* **2010**, *6*, 663−669.

(24) Zhu, C.; Liu, L.; Yang, Q.; Lv, F.; Wang, S. Water-soluble conjugated polymers for imaging, diagnosis, and therapy. *Chem. Rev.* **2012**, *112*, 4687−4735.

(25) Wang, S.; Gaylord, B. S.; Bazan, G. C. Fluorescein provides a resonance gate for FRET from conjugated polymers to DNA intercalated dyes. *J. Am. Chem. Soc.* **2004**, *126*, 5446−5451.

(26) Mai, C.-K.; Schlitz, R. A.; Su, G. M.; Spitzer, D.; Wang, X.; Fronk, S. L.; Cahill, D. G.; Chabinyc, M. L.; Bazan, G. C. Side-chain effects on the conductivity, morphology, and thermoelectric properties of self-doped narrow-band-gap conjugated polyelectrolytes. *J. Am. Chem. Soc.* **2014**, *136*, 13478−13481.

(27) Henson, Z. B.; Zhang, Y.; Nguyen, T.-Q.; Seo, J. H.; Bazan, G. C. Synthesis and properties of two cationic narrow band gap conjugated polyelectrolytes. *J. Am. Chem. Soc.* **2013**, *135*, 4163−4166.

(28) Mai, C. K.; Zhou, H.; Zhang, Y.; Henson, Z. B.; Nguyen, T. Q.; Heeger, A. J.; Bazan, G. C. Facile doping of anionic narrow-band-gap conjugated polyelectrolytes during dialysis. *Angew. Chem., Int. Ed.* **2013**, *52*, 12874−12878.

(29) Yang, R.; Garcia, A.; Korystov, D.; Mikhailovsky, A.; Bazan, G. C.; Nguyen, T.-Q. Control of interchain contacts, solid-state fluorescence quantum yield, and charge transport of cationic conjugated polyelectrolytes by choice of anion. *J. Am. Chem. Soc.* **2006**, *128*, 16532−16539.

(30) Yang, R.; Wu, H.; Cao, Y.; Bazan, G. C. Control of cationic conjugated polymer performance in light emitting diodes by choice of counterion. *J. Am. Chem. Soc.* **2006**, *128*, 14422−14423.

(31) Cheng, Y.-J.; Yang, S.-H.; Hsu, C.-S. Synthesis of conjugated polymers for organic solar cell applications. *Chem. Rev.* **2009**, *109*, 5868−5923.

(32) Li, G.; Zhu, R.; Yang, Y. Polymer solar cells. *Nat. Photonics* **2012**, *6*, 153−161.

(33) Facchetti, A. π-Conjugated polymers for organic electronics and photovoltaic cell applications. *Chem. Mater.* **2011**, *23*, 733−758.

(34) Seo, J. H.; Namdas, E. B.; Gutacker, A.; Heeger, A. J.; Bazan, G. C. Solution-processed organic light-emitting transistors incorporating conjugated polyelectrolytes. *Adv. Funct. Mater.* **2011**, *21*, 3667−3672.

(35) Ikenoue, Y.; Outani, N.; Patil, A.; Wudl, F.; Heeger, A. Electrochemical studies of self-doped conducting polymers: verification of the 'cation-popping'doping mechanism. *Synth. Met.* **1989**, *30*, 305−319.

(36) Ionescu-Zanetti, C.; Mechler, A.; Carter, S. A.; Lal, R. Semiconductive polymer blends: correlating structure with transport properties at the nanoscale. *Adv. Mater.* **2004**, *16*, 385−389.

(37) Nardes, A. M.; Kemerink, M.; Janssen, R. A.; Bastiaansen, J. A.; Kiggen, N. M.; Langeveld, B. M.; Van Breemen, A. J.; De Kok, M. M. Microscopic understanding of the anisotropic conductivity of PEDOT: PSS thin films. *Adv. Mater.* **2007**, *19*, 1196−1200.

(38) De Jong, M.; Van Ijzendoorn, L.; De Voigt, M. Stability of the interface between indium-tin-oxide and poly (3, 4-ethylenedioxythiophene)/poly (styrenesulfonate) in polymer light-emitting diodes. *Appl. Phys. Lett.* **2000**, *77*, 2255−2257.

(39) Wong, K. W.; Yip, H.; Luo, Y.; Wong, K.; Lau, W.; Low, K.; Chow, H.; Gao, Z.; Yeung, W.; Chang, C. Blocking reactions between indium-tin oxide and poly (3, 4-ethylene dioxythiophene): poly (styrene sulphonate) with a self-assembly monolayer. *Appl. Phys. Lett.* **2002**, *80*, 2788−2790.

DOI: 10.1021/acs.accounts.7b00501
Acc. Chem. Res. 2018, 51, 202−211

(40) Pingree, L. S.; MacLeod, B. A.; Ginger, D. S. The changing face of PEDOT: PSS films: Substrate, bias, and processing effects on vertical charge transport. *J. Phys. Chem. C* **2008**, *112*, 7922−7927.
(41) Zhou, H.; Zhang, Y.; Mai, C.-K.; Collins, S. D.; Nguyen, T.-Q.; Bazan, G. C.; Heeger, A. J. Conductive conjugated polyelectrolyte as hole-transporting layer for organic bulk heterojunction solar cells. *Adv. Mater.* **2014**, *26*, 780−785.
(42) Zhou, H.; Zhang, Y.; Mai, C.-K.; Collins, S. D.; Bazan, G. C.; Nguyen, T.-Q.; Heeger, A. J. Polymer homo-tandem solar cells with best efficiency of 11.3%. *Adv. Mater.* **2015**, *27*, 1767−1773.
(43) Choi, H.; Mai, C.-K.; Kim, H.-B.; Jeong, J.; Song, S.; Bazan, G. C.; Kim, J. Y.; Heeger, A. J. Conjugated polyelectrolyte hole transport layer for inverted-type perovskite solar cells. *Nat. Commun.* **2015**, *6*, 7348.
(44) Lu, L.; Rininsland, F. H.; Wittenburg, S. K.; Achyuthan, K. E.; McBranch, D. W.; Whitten, D. G. Biocidal activity of a light-absorbing fluorescent conjugated polyelectrolyte. *Langmuir* **2005**, *21*, 10154−10159.
(45) Chemburu, S.; Corbitt, T. S.; Ista, L. K.; Ji, E.; Fulghum, J.; Lopez, G. P.; Ogawa, K.; Schanze, K. S.; Whitten, D. G. Light-induced biocidal action of conjugated polyelectrolytes supported on colloids. *Langmuir* **2008**, *24*, 11053−11062.
(46) Ding, L.; Chi, E. Y.; Schanze, K. S.; Lopez, G. P.; Whitten, D. G. Insight into the mechanism of antimicrobial conjugated polyelectrolytes: lipid headgroup charge and membrane fluidity effects. *Langmuir* **2010**, *26*, 5544−5550.
(47) Yuan, H.; Liu, Z.; Liu, L.; Lv, F.; Wang, Y.; Wang, S. Cationic conjugated polymers for discrimination of microbial pathogens. *Adv. Mater.* **2014**, *26*, 4333−4338.
(48) Zhu, C.; Yang, Q.; Liu, L.; Wang, S. Visual optical discrimination and detection of microbial pathogens based on diverse interactions of conjugated polyelectrolytes with cells. *J. Mater. Chem.* **2011**, *21*, 7905−7912.
(49) Zhu, C.; Yang, Q.; Liu, L.; Lv, F.; Li, S.; Yang, G.; Wang, S. Multifunctional cationic poly (p-phenylene vinylene) polyelectrolytes for selective recognition, imaging, and killing of bacteria over mammalian cells. *Adv. Mater.* **2011**, *23*, 4805−4810.
(50) Feng, G.; Mai, C.-K.; Zhan, R.; Bazan, G. C.; Liu, B. Narrow band gap conjugated polyelectrolytes for photothermal killing of bacteria. *J. Mater. Chem. B* **2015**, *3*, 7340−7346.
(51) Snyder, G. J.; Toberer, E. S. Complex thermoelectric materials. *Nat. Mater.* **2008**, *7*, 105−114.
(52) Du, Y.; Shen, S. Z.; Cai, K.; Casey, P. S. Research progress on polymer−inorganic thermoelectric nanocomposite materials. *Prog. Polym. Sci.* **2012**, *37*, 820−841.
(53) See, K. C.; Feser, J. P.; Chen, C. E.; Majumdar, A.; Urban, J. J.; Segalman, R. A. Water-processable polymer−nanocrystal hybrids for thermoelectrics. *Nano Lett.* **2010**, *10*, 4664−4667.
(54) Poehler, T. O.; Katz, H. E. Prospects for polymer-based thermoelectrics: state of the art and theoretical analysis. *Energy Environ. Sci.* **2012**, *5*, 8110−8115.
(55) Dubey, N.; Leclerc, M. Conducting polymers: Efficient thermoelectric materials. *J. Polym. Sci., Part B: Polym. Phys.* **2011**, *49*, 467−475.
(56) Bubnova, O.; Crispin, X. Towards polymer-based organic thermoelectric generators. *Energy Environ. Sci.* **2012**, *5*, 9345−9362.
(57) Zhang, Q.; Sun, Y.; Xu, W.; Zhu, D. Organic thermoelectric materials: emerging green energy materials converting heat to electricity directly and efficiently. *Adv. Mater.* **2014**, *26*, 6829−6851.
(58) Choy, C. L. Thermal conductivity of polymers. *Polymer* **1977**, *18*, 984−1004.
(59) Cheng, F.; Imin, P.; Lazar, S.; Botton, G. A.; de Silveira, G.; Marinov, O.; Deen, J.; Adronov, A. Supramolecular functionalization of single-walled carbon nanotubes with conjugated polyelectrolytes and their patterning on surfaces. *Macromolecules* **2008**, *41*, 9869−9874.
(60) Casagrande, T.; Imin, P.; Cheng, F.; Botton, G. A.; Zhitomirsky, I.; Adronov, A. Synthesis and electrophoretic deposition of single-walled carbon nanotube complexes with a conjugated polyelectrolyte. *Chem. Mater.* **2010**, *22*, 2741−2749.
(61) Li, Y.; Mai, C.-K.; Phan, H.; Liu, X.; Nguyen, T.-Q.; Bazan, G. C.; Chan-Park, M. B. Electronic properties of conjugated polyelectrolyte/single-walled carbon nanotube composites. *Adv. Mater.* **2014**, *26*, 4697−4703.
(62) Kong, J.; Franklin, N. R.; Zhou, C.; Chapline, M. G.; Peng, S.; Cho, K.; Dai, H. Nanotube molecular wires as chemical sensors. *Science* **2000**, *287*, 622−625.
(63) Bradley, K.; Jhi, S.-H.; Collins, P. G.; Hone, J.; Cohen, M. L.; Louie, S. G.; Zettl, A. Is the Intrinsic thermoelectric power of carbon nanotubes positive? *Phys. Rev. Lett.* **2000**, *85*, 4361−4364.
(64) Collins, P. G.; Bradley, K.; Ishigami, M.; Zettl, A. Extreme oxygen sensitivity of electronic properties of carbon nanotubes. *Science* **2000**, *287*, 1801−1804.
(65) Mai, C.-K.; Russ, B.; Fronk, S. L.; Hu, N.; Chan-Park, M. B.; Urban, J. J.; Segalman, R. A.; Chabinyc, M. L.; Bazan, G. C. Varying the ionic functionalities of conjugated polyelectrolytes leads to both p- and n-type carbon nanotube composites for flexible thermoelectrics. *Energy Environ. Sci.* **2015**, *8*, 2341−2346.
(66) Mai, C.-K.; Liu, J.; Evans, C. M.; Segalman, R. A.; Chabinyc, M. L.; Cahill, D. G.; Bazan, G. C. Anisotropic thermal transport in thermoelectric composites of conjugated polyelectrolytes/single-walled carbon nanotubes. *Macromolecules* **2016**, *49*, 4957−4963.
(67) Brus, V. V.; Gluba, M. A.; Mai, C.-K.; Fronk, S. L.; Rappich, J.; Nickel, N. H.; Bazan, G. C. Conjugated polyelectrolyte/graphene hetero-bilayer nanocomposites exhibit temperature switchable type of conductivity. *Adv. Electron. Mater.* **2017**, *3*, 1600515.

DOI: 10.1021/acs.accounts.7b00501
Acc. Chem. Res. 2018, 51, 202−211